This paper first appeared in the eleventh print edition of *Photovoltaics International* journal, published in February 2011.

Processing of highly-efficient MWT silicon solar cells

F. Clement[1], **M. Neidert**[2], **A. Henning**[2], **C. Mohr**[2], **W. Zhang**[2], **B. Thaidigsmann**[1], **R. Hoenig**[1], **T. Fellmeth**[1], **A. Spribille**[1], **E. Lohmueller**[1], **A. Krieg**[1], **M. Glatthaar**[1], **H. Wirth**[1], **D. Biro**[1], **R. Preu**[1], **M. Menkoe**[3], **K. Meyer**[3], **D. Lahmer**[3] & **H.-J. Krokoszinski**[3]
[1]Fraunhofer ISE, Freiburg, Germany; [2]Heraeus Precious Metal, Hanau, Germany; [3]Bosch Solar Energy AG, Erfurt, Germany

ABSTRACT
This paper focuses on the latest developments from research on MWT (metal wrap-through) solar cells at Fraunhofer ISE. An overview of the current cell results for mc-Si and Cz-Si material with both Al-BSF and passivated rear side is presented. Recent progress in cell technology and challenges to reaching efficiencies of 20% for industrially processed large-area MWT solar cells are also discussed. Up to recently, MWT cell efficiencies of up to 19% for Cz-Si and up to 17.5% for mc-Si have been reached with industrially feasible processing. Improvements to the design of the MWT cell to increase cell efficiency and to allow an easy module assembly are also presented in this paper, as are first calibrated IV measurements of MWT solar cells.

Introduction
The most common industrial cell and module production approaches are mainly based on screen-printed H-patterned silicon solar cells. Therefore, today's modules suffer from high front-surface shading and from series resistance losses in the tabbing material. Both loss mechanisms are caused by the presence of an external contact, the so-called busbar, on the front surface. To reduce these losses significantly, the busbar has to be transferred to the rear surface. This can be realized by metal wrap-through (MWT) technology [1] while using only industrially-applicable production technologies [2]. The main advantage of the MWT technology among the rear-contact cell technologies is its need for only two additional process steps for cell production in comparison to conventional technology, which requires laser via drilling and rear-contact isolation. The via-metallization can be done in the same process step as the rear-solder pad metallization [3].
Hence, the MWT technology allows high efficiencies [4–6, 8] while production costs are still on a low level. Therefore the costs per Wp can be reduced at low economical risks. The transfer of the MWT technology from laboratory to industry is already ongoing and has been successful so far [3, 7–9]. This paper presents a detailed overview of the current status of MWT research and development at the PV-TEC pilot-line [10, 11] at Fraunhofer ISE, focusing on recent progress in cell processing and characterization.

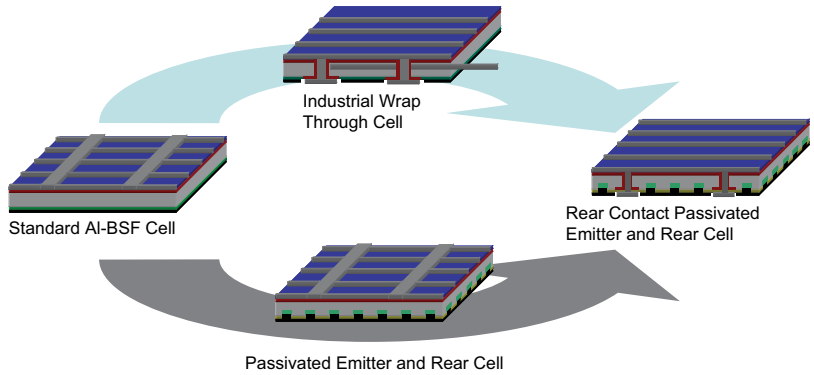

Figure 1. Fraunhofer ISE technology roadmap for future cell devices.

Furthermore, the combination of the MWT technology with rear surface passivation is presented. The combination of industrial wrap-through cell technologies like the MWT technology with passivated emitter and rear cell (PERC) technologies is the most important part of the technology roadmap of Fraunhofer ISE (see Fig. 1) in order to improve cell efficiencies for large-area lab-scale series-processed solar cells

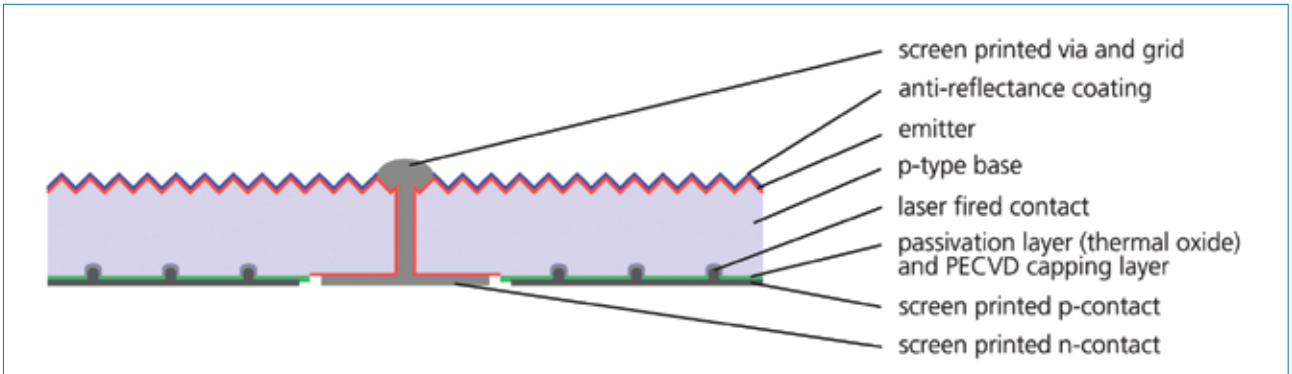

Figure 2. Schematic structure of the MWT-PERC devices presented in this work.

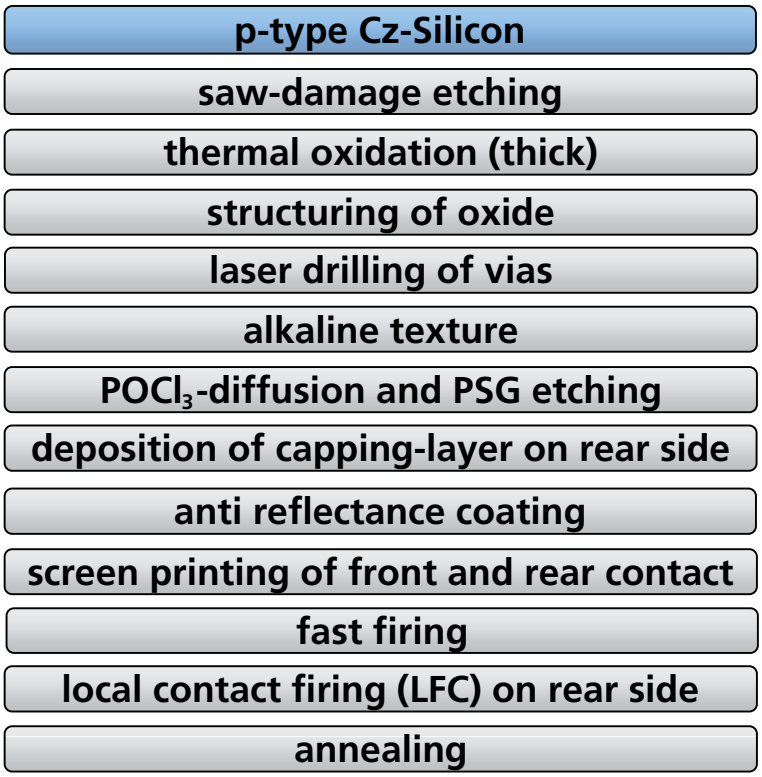

Figure 3. Process sequence for the fabrication of Cz-Si MWT-PERC devices.

towards 20%. The so-called MWT-PERC approach should enable a clear increase in cell efficiency.

Approach

In order to develop a highly-efficient MWT solar cell and module technology on a cost-efficient level, we have chosen to use a multi-stage approach. On the one hand we focus on the development of an MWT pilot-line process for industrial mc- and Cz-Si material which can be transferred to industry in a short timeframe. On the other hand, we have developed an industrially feasible process with a very high-efficiency potential (over 19%) on FZ-Si [12] in order to characterize MWT cells in detail and thus to improve processing of MWT cells.

Moreover, we successfully finished our first experiments with screen-printed MWT-PERC devices (see Fig. 2) on mc-Si and Cz-Si by applying a dielectrical layer, e.g. silicon oxide [13, 14] or aluminium oxide [15–17], on the rear surface. Cell thicknesses down to ~120µm are realized with the MWT-PERC approach without any bowing effects, thus producing high yield. A typical process sequence for the MWT-PERC approach with thermal oxide as the rear passivation layer is presented in Fig. 3. In this approach, the oxide also acts as the masking layer during diffusion and texturing processes. Within this work, cell processing of Cz-Si MWT-PERC devices is based on this process sequence, shown in Fig. 2. Additionally, for some MWT cells the front metallization was performed by a seed and plate approach with aerosol jetting for seed-layer formation followed by light-induced silver plating (LIP) [18]. More details about Cz-Si MWT-PERC devices are available in literature [19].

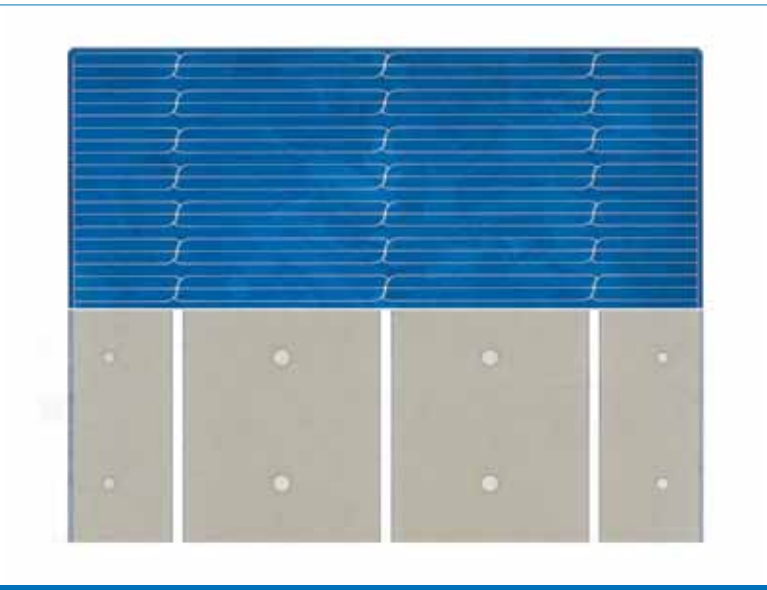

Figure 4. Front and rear of a typical mc-MWT solar cell (156 × 156 mm^2) with three continuous rear busbars processed at Fraunhofer ISE [25].

For mc-Si MWT-PERC devices, a process based on aluminium oxide – deposited by PECVD – as rear passivation layer and screen-printed front and rear contacts is used within this work. Results of aluminium oxide processing and characterization work at Fraunhofer ISE can be found in [15–17]. In order to protect the Al_2O_3 passivation layer from the screen-printed aluminium rear contact during the contact firing, an SiN capping layer is applied by PECVD on the rear side. The rear-side emitter is structured by a diffusion barrier. The backend processing (ARC deposition and so on) is similar to the process sequence presented in Fig. 3.

Screen-printing pastes for the front and via-metallization are developed in a joint project with Heraeus to ensure high cell efficiencies. The development of the via-metallization paste is of particularly high importance in order to reduce shunting and series resistance losses in the via-contact and therefore to optimize MWT cell processing. More details about current results with mc-Si MWT cells and the challenges of the MWT via paste development were presented by R. Hoenig and M. Neidert [20, 21].

Processing of the MWT cells employed the PV-TEC pilot-line [10]. In the case of Cz-Si MWT cell processing with aluminium back-surface field (Al-BSF), the experiments were carried out mainly at the PV lab of Bosch Solar Energy AG [9, 22]. An MWT layout with three continuous rear busbars (see Fig. 4) is used for all MWT cells unless specified otherwise.

In order to confirm the advantages of the MWT technology on the module level, MWT prototype modules were processed and compared to conventional modules as a first step. New MWT cell designs are under development with partners from the cell and module industry to ensure ease of module assembly [23].

A new inline processing-capable measurement system was developed to aid in delivering high-precision and fast IV measurements for MWT cells, which were in turn fixated during the IV measurement by use of vacuum [24]. First calibrated IV measurements performed

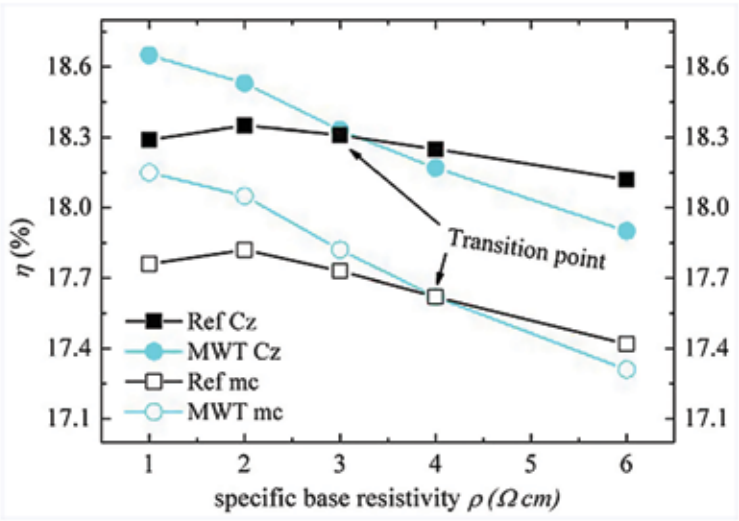

Figure 5. 2D "Sentaurus Device" simulation of an MWT and conventional solar cell [26]. The simulation shows a transition point depending on the bulk lifetime (mc, Cz) and base resistivity. Boron oxygen-induced degradation effects of the bulk lifetime are disregarded. The absolute values for the bulk lifetime are based on estimated input parameters; in the case of mc-Si in particular, an overestimation is likely.

at the Fraunhofer ISE CalLab PV Cells are presented in the coming sections.

Furthermore, loss mechanisms in MWT cells (e.g. losses due to via resistance [24], lateral base resistance [2], J_0-related recombination [3], etc.) have to be analyzed and minimized. A 2D simulation, as shown in Fig. 5, was carried out by the so-called "Sentaurus device" in order to clarify the origin of MWT loss mechanisms. In Fig. 5, the calculated efficiency is plotted against the base resistivity for low (mc-Si) and high (Cz-Si) bulk lifetime. The simulation is based on the design of a typical MWT solar cell (156 × 156mm^2) with three rear busbars without interruptions as shown in Fig. 4, using a conventional H-patterned solar cell with three busbars as a reference (indicated by 'Ref' in the graph legend).

Fig. 5 shows that a high efficiency gain can be achieved for MWT cells, especially for mc-Si with low base resistivity (< 2Ωcm). For Cz-Si cells, especially for those with high base resistivity (> 3Ωcm), the cell design shown in Fig. 4 leads to efficiency losses for MWT cells caused by lateral resistance losses in the base and by recombination losses in the rear n-contact region [26]. Hence, either the base resistivity has to be reduced or the rear MWT cell design must be optimized to achieve an efficiency gain. One possibility for an optimization of the cell design is presented in this work; others are discussed by K. Meyer [22].

Results and discussion

Most current-voltage (I-V) measurements are carried out using newly developed measurement equipment [24]. All cell measurements are performed by an industrial cell tester; best cells are partly measured by the Fraunhofer ISE CalLab PV Cells.

Results for MWT Cell with Al-BSF

Table 1 lists the best results of MWT cells with aluminium BSF rear side. The mean difference (Δ) when compared to conventionally processed solar cells is also presented for all IV parameters in absolute values. For a precise comparison, only sister wafers are used.

Device type	V_{oc}(mV)	J_{sc}(mA/cm²)	*FF*(%)	η(%)
mc-Si[1]	614	34.9	78.3	**16.8**
Δ(mc-Si)	+2	+1.0	-0.5	**+0.5**
Cz-Si[1]	619	37.2	77.2	17.7
Δ(Cz-Si)	0	+0.9	-1.6	0
Cz-Si[2] (new)	626	37.8	77.0	**18.2**
Δ(Cz-Si new)	+3	+1.0	-1.0	**+0.3**

[1]Independently confirmed by Fraunhofer ISE CalLab PV Cells (after degradation); measurement uncertainty: ±2%rel. for η.
[2]I-V measurements with cell tester after processing, measurement uncertainty: ±3%rel. for η.

Table 1. I-V data for the best MWT cells with Al-BSF rear measured on an industrial cell tester and partly independently confirmed by the Fraunhofer ISE CalLab PV Cells. The mean difference Δ to conventionally processed solar cells (sister wafers) is also presented (absolute values). The Cz-Si results labelled 'new' are based on a new rear-side design. The cell area is 156 × 156mm²; base resistivity for mc-Si is ~0.5–2.0Ωcm, for Cz-Si ~2–4Ωcm.

Device type	V_{oc}(mV)	J_{sc}(mA/cm²)	*FF*(%)	η(%)
mc-Si (~130µm)[1]	628	36.0	76.6	17.3
mc-Si (~130µm)[2]	630	36.0	76.9	17.5
Cz-Si (~120µm)[2]	628	39.0	75.9	18.6
Cz-Si (~170µm)[2]	630	39.9	74.8	18.8
	seed and plate approach (front contact):			
Cz-Si (~170µm)[2]	639	40.3	73.6	19.0

[1]Independently confirmed by Fraunhofer ISE CalLab PV Cells (after degradation); measurement uncertainty: ±2%rel. for η.
[2]I-V measurements with cell tester after processing, measurement uncertainty: ±3%rel. for η.

Table 2. I-V-data for the best MWT-PERC cells with passivated rear side measured on an industrial cell tester and partly independently confirmed by the Fraunhofer ISE CalLab PV Cells. The cell area is 125 × 125mm² for Cz-Si and 156 × 156mm² for mc-Si. The cell thickness after processing is given in brackets. The base resistivity for mc-Si is ~0.8Ωcm; for Cz-Si it is 1.7Ωcm (~120µm) and 2.7Ωcm (~170µm). For one Cz-Si group, the seed and plate approach was used for front metallization.

For mc-Si, a sufficient efficiency level (up to 16.8%) is reached. However, the moderate voltage level indicates that the used mc-Si material does not have the highest material quality. Nevertheless, a clear efficiency gain of 0.5% absolute (~3% rel.) is achieved with the MWT cell technology. The estimated efficiency gain in Fig. 5 (~0.5% at 1Ωcm) is confirmed. This underlines the high potential of the MWT concept for mc-Si material.

For Cz-Si material (~2–4Ωcm), the efficiency level is ~1% absolute higher than for mc-Si as expected, but no significant efficiency gain can be observed for MWT cells with three continuous rear busbars (cell design as presented in Fig. 4). A similar behaviour is shown by the simulations that were carried out (see Fig. 5). For Cz-Si material with a base resistivity of ~3Ωcm, no efficiency increase is expected for the MWT approach. The reasons for this behaviour are discussed in detail in [26]. A main reason is the rear busbar region without p-contact (Al-BSF), which leads to significant FF losses especially for high-quality material with high base resistivity. Due to strong boron oxygen-induced degradation effects for a low base resistivity, the Cz-Si base material remains unchanged; however, a modification of the rear busbar region can significantly improve the FF for MWT cells [26]. Therefore, the MWT rear design was optimized, and the rear n-contact region was significantly reduced.

A new MWT cell batch ('Cz-Si new' in Table 1) was processed with an optimized rear design, resulting in efficiencies up to 18.2%. This is so far the highest MWT efficiency achieved for AL-BSF rear sides within this work. Due to the rear design optimization, an efficiency gain of about 0.3% absolute (~1.7% rel.) mainly based on decreased fill factor losses is observed for MWT cells. Hence, the high potential of the MWT concept is also shown for Cz-Si material.

Device type	V_{oc}(V)	J_{sc}(mA/cm²)	Δ*FF*(%)	Δη(%)
MWT	3.64	35.6	-3.8	-1.3
Conv.	3.60	34.4	-5.5	-1.5
Δ(MWT-Conv.)	+0.04	+1.2	+.1.7	+0.2

Table 3. I-V results of a comparison of an MWT and a conventional Cz-Si mini-module (each consisting of six cells). ΔFF and Δη signify the following differences in % absolute: FF/η (module) minus FF/η (cell); measurement uncertainty: ±3%rel. for η.

Results for passivated MWT cells (MWT-PERC)

To improve cell efficiencies further, the MWT cell concept is combined with the PERC concept [19] as described earlier. The results of the best so-called MWT-PERC devices are listed in Table 2.

For mc-Si material, sufficient efficiencies up to 17.3% are reached in the first run. Hence, an efficiency gain compared to the Al-BSF approach of about 0.5% absolute (~3% rel.) is achieved due to rear-side passivation. Further cell batches including the mentioned optimization of the MWT rear design are already in process focusing cell efficiencies towards 18%.

Thus far, Cz-Si materials reached efficiencies of up to 18.8% within the first runs using screen-printed front and rear contacts. With the seed (aerosol jetting [27]) and plate (Ag-LIP) approach for the front contact, efficiencies of 19.0% were achieved, leading to the conclusion that the MWT efficiency is increased by over 0.5% absolute (>3% rel.) due to rear-side passivation. The slightly increased efficiency for the thicker Si material can most likely be explained by an optimized front grid which was used in this batch and by more effective light capturing due to the thicker base material. Both effects lead to a clear increase in J_{sc}. The FF decrease for the thicker Cz-Si can be explained by the higher base resistivity (see Fig. 5). The gain in both J_{sc} and V_{oc} as well as the FF loss for the seed and plate approach can be explained by a reduction of the finger width (reduced shading) and by the use of an emitter with higher sheet resistance.

The next cell batches should see efficiencies in the region of 20% either by the use of higher doped base material and/or by the mentioned optimization of the MWT rear-side design, coupled with the introduction of the seed and plate approach for the front contact. The final cell thicknesses of ~120µm show the feasibility of the MWT-PERC approach to be used for industrial processing of very thin mc-Si and Cz-Si wafer material.

MWT module results

Two mini modules (one MWT and one conventional), each consisting of six Cz-Si solar cells, were processed [9]; Table 3 displays the I-V results for both modules. An efficiency increase of ~0.2% absolute (~1.5% rel.) is reached on the module level for the MWT technology. This increase is driven by the decrease of series resistance losses due to an optimized MWT tabbing technology, which allows more tabbing material on the rear without additional shading. The reduced FF difference (ΔFF) for the MWT technology confirms the reduction of the series resistance losses on the module level. The clear increase in J_{sc} for the MWT technology can be explained by less shading due the absence of front busbars and tabs.

Mini-modules with very thin (~120µm) MWT-PERC devices were processed first. For the Cz-Si material, module efficiencies of ~16.5% were achieved. The moderate value can thus far be explained by a non-optimized MWT rear side for module interconnection. Further experiments with an optimized MWT rear design are already underway; further details regarding module technology for back-contacted solar cells are presented in [23].

Conclusion

We demonstrated the industrial fabrication of large-area metal wrap-through silicon solar cells with Al-BSF rear sides as well as with passivated rear surfaces (MWT-PERC approach) in our PV-TEC pilot-line using Cz- and mc-Si material. For mc-Si MWT cells with Al-BSF, an efficiency gain of about 0.5% absolute is achieved compared to conventionally processed cells (sister wafers). For Cz-Si materials, efficiencies up to 18.2% are achieved with an optimized rear side with less rear n-contact metallization. Hence, the high potential of the MWT concept has been illustrated on both materials.

MWT-PERC devices reached efficiencies of up to 19.0% on Cz-Si and up to 17.5% on mc-Si, confirming the high efficiency level which is achievable with the MWT-PERC approach. Moreover, MWT-PERC devices with thicknesses down to ~120µm are successfully processed on industrial equipment, showing the high cost reduction potential of the MWT-PERC concept for very thin wafer material.

A further efficiency gain for the MWT technology is demonstrated on the module level by using an optimized MWT tabbing technology. To achieve MWT efficiencies towards 20%, two main strategies were selected. Firstly, an optimization of the MWT rear-side design, which is mainly based on the reduction of the rear n-contact area, will increase the MWT efficiency. Secondly, the use of wafer material with low base resistivity will push the MWT efficiencies further if boron oxygen-induced degradation effects can be neglected.

Acknowledgements

The authors would like to thank all co-workers at the Photovoltaic Technology Evaluation Center (PV-TEC) at Fraunhofer ISE, at Bosch Solar Energy AG and at Heraeus's PV business unit for processing and characterizing the samples. This work was partly funded within the seventh framework programme of the European Union under contract no. 218966 (ULTIMATE) as well as by the German Federal Ministry for the Environment, Nature Conservation and Reactor Safety under project no. 0329849B.

References

[1] van Kerschaver, E. et al. 1998, *Proc. 2nd WCPEC*, Vienna, Austria, p. 1479.
[2] Clement, F. et al. 2009, *Solar Energy Materials & Solar Cells*, Vol. 93, p. 1051.
[3] Clement, F. et al. 2009, Proc. *34th IEEE PVSC*, Philadelphia, USA, p. 1.
[4] Clement, F. et al. 2009, *Proc. 24th EU PVSEC*, Hamburg, Germany, p. 2172.
[5] Inoue, S. et al. 2008, *Proc. 23rd EU PVSEC*, Valencia, Spain, p. 1.
[6] Bennett, I.J. et al. 2009, *Proc. 24th EU PVSEC*, Hamburg, Germany, p. 3258.
[7] van den Donker, M.N. et al. 2008, *Proc. 23rd EU PVSEC*, Valencia, Spain, p. 1.
[8] Dross, F. et al. 2007, *Technical Digest 17th Int. PVSEC*, Fukuoka, Japan, p. 410.
[9] Lahmer, D. et al. 2009, *Proc. 24th EU PVSEC*, Hamburg, Germany, p. 2168.
[10] Biro, D. et al. 2006, *Proc. 21st EU PVSEC*, Dresden, Germany, p. 621.
[11] Biro, D. et al. 2009, *Proc. 24th EU PVSEC*, Hamburg, Germany, p. 1901.
[12] Fellmeth, T. et al. 2009, *Proc. 24th EU PVSEC*, Hamburg, Germany, p. 711.
[13] Biro, D. et al. 2009, *Proc. 34th IEEE PVSC*, Philadelphia, USA, p. 1594.
[14] Mack, S. et al. 2009, *Proc. 24th EU PVSEC*, Hamburg, Germany, p. 1574.
[15] Saint-Cast, P. et al. 2009, *Applied Physics Letters*, Vol. 95, p. 151502.
[16] Kania, D. et al. 2009, *Proc. 24th EU PVSEC*, Hamburg, Germany, p. 2275.
[17] Saint-Cast, P. et al. 2010, *IEEE Electron Device Letters*, Vol. 31, p. 695.
[18] Hoerteis, M. 2009, Ph.D. thesis, University of Constance.
[19] Thaidigsman, B. et al. 2010, *Proc. 25th EU PVSEC*, Valencia, Spain.
[20] M. Neidert, et al., *Proc. 24th EU PVSEC*, Hamburg, Germany, p. 1424.
[21] Hoenig, R. et al. 2010, *Proc. 35th IEEE PVSC*, Honolulu, Hawaii, USA.
[22] Meyer, K. et al. 2010, *Proc. 25th EU PVSEC*, Valencia, Spain.
[23] Wirth, H. et al. 2010, *Proc. 25th EU PVSEC*, Valencia, Spain.
[24] Glatthaar, M. et al. 2010, *Proc. 25th EU PVSEC*, Valencia, Spain.
[25] Clement, F. et al. 2009, *Solar Energy Materials & Solar Cells*, Vol. 94, p. 51.
[26] Fellmeth, T. et al. 2010, *Proc. 25th EU PVSEC*, Valencia, Spain.

Enquiries

W.C. Heraeus GmbH
Thick Film Materials Division
Heraeusstr. 12-14
63450 Hanau
Germany

Fraunhofer Institute for Solar Energy Systems (ISE)
Heidenhofstr. 2
79110 Freiburg
Germany

Bosch Solar Energy AG
Wilhelm-Wolff-Str. 23
99099 Erfurt
Germany

Email: florian.clement@ise.fraunhofer.de